韓國海岸海洋工學發表論文集 (2003)
第14券, pp. 143-153

Perturbation in Yellow Sea Tidal Current Regime due to Barrier Construction at Saemangeum
새만금 방조제 건설에 의한 황해 조류체계의 교란

Byung Ho Choi[1] and Han Soo Lee[1]
최병호[1] · 이한수[1]

1. INTRODUCTION

The necessity of predicting changes in tidal regime that would be caused by large coastal engineering developments has been led to increased numerical modeling of tides on the continental shelf since 1970s (Flather 1976; Choi 1978; Greenberg 1979). The aim of this study was to predict how the construction of tidal barriers in the region of the Yellow sea and the East China Sea continental shelf would disturb and/or alter the system's natural tidal state.Because of high project costs, and in view of the possible environmental consequences, itis important that correct evaluations are made. The only practical way of obtaining this good approximate solution is to construct a mathematical model that simulates the behavior of the tidal system, which play the central role in the shelf sea, involving a set of equations of motion of the sea that are solved numerically to yield the tidal variation. The proposed changes in boundary configuration due to barrier scheme can then be inserted in the model and the resultant effects on the system estimated. The degree of confidence of these approximations is a function of accuracy with which the model reproduces the real system. During the past years, this approach has been widely used for the studies of barrier schemes in the Bristol Channel (Heaps 1972; Miles1979; Owen and Heaps 1979), the Bay of Fundy (Garett 1972; Greenberg 1979; Duff 1979) and the west coast of Korea (Choi 1978, 1981, 2001). One of the most difficult and important tasks in this approach is that a sufficiently large region should be considered in the mathematical modeling since good results may only be expected by locating the open boundaries sufficiently far from the barrier sites beyond the barrier's influence. Some previous studied in this nature (Heaps and Greenberg 1974; Garrett and Greenberg 1977) indicate that unreasonable results may be obtained if too small a sea area is considered in the computations.

2. GEOGRAPHICAL SETTING

Mangyong-Geum (Mangeum) estuary is a relatively shallow macrotidal embayment (the average tidal range is 5.7 m on springs and 2.8 m on neaps) located at latitude 35 °N of the western coast of Korean Peninsula in the eastern Yellow Sea as shown in Fig. 1. Its maximum depth is 10 m (below Indian Spring Low) at the mouth of the Geum estuary and it also has a broad intertidal zone exposed during the tide. In common with other estuaries in the western coast of Korea, tidal currents have a profound influence on the sediment dynamics in the area. The severe winter storms arising from northwesterly winds also create strong current. Therefore tide and wave conditions of sufficient intensity categorize this area as a high energy

[1] Department of Civil and Environmental Engineering, Sungkyunkwan University, Suwon 440-746, Korea
bhchoi@skku.edu, ban8303@skku.edu

environment.

In this sea area Saemangeum tidal barrier has been constructed since 1991 connecting offshore islands from Bieung and Osic Islands at southern Geum estuary to Daehangri at southern Mangyong estuary to form 40,100ha reclamation area and freshwater reservoir. As of June, 2003 30.3kilometers of barrier was constructed among total of 33 kilometers leaving openings of 1.1 kilometers at Sinsi Island gate construction area and 1.6 kilometers at near Garyuck Island. About 1.8 kilometers of openings between Yami and Bieung Islands which is for convenience, classified as Number Four Dike have been closed recently

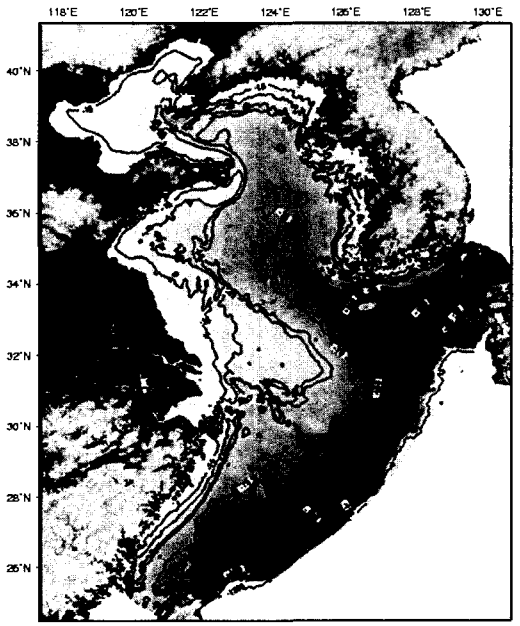

Fig. 1. Bathymetry of whole model domain in East China and Yellow Sea.

Locally significant bed changes due to sand movement have been reported previously along the dike alignment between Osik and Yami Islands (Choi, 2001). The sandbank-like deposition has been occurred at originally-planned closure site at Number 4 dike between Yami and Bieung Island recording rapid sand deposition of 4-5 meters along the dike alignment at about two kilometers distance. Choi(2001) reported that this bottom evolution with sands is somewhat faster than hydrodynamic interpretation of Huthnance (1982). So the region is not only remarkable features in turbid suspended sediment movement as manifested in the satellite images but long term bed morphological changes due to bedload transport also may play an important role in sediment dynamics in the region. In northern part of Saemangeum dikes, an extensive port development is being progressed by constructing parallel dike and quay walls at Keum estuary. Although the project has been started with optimistic view that sediment supply from upstream river will significantly decrease by damming the upstream river, however considerable amount of siltation has begun in the channel, possibly due to redistribution of sediment within the estuary with continuous suspended sediment supply from outer estuary along the coast especially during winter monsoon.

3. REGIONAL TIDE SIMULATOR

Investigation of the tides in the East Asian Seas started during the late 1970s with the formulation of a two-dimensional model for basic studies of tidal propagation in the Yellow Sea and the East China Sea continental shelf (Choi, 1980). This has been followed by a series of studies aimed at predicting tidal changes due to tidal barriers for potential tidal power exploitation, land reclamation and port development using a combination of the Yellow Sea model and estuarine tidal models. A modeling technique that converts the model equations to be a discrete form and allows computation over spatially unstructured meshes has been used to set up as a main component of regional ocean tide simulator taking the advantage of more accurate representation of the coastlines, coastal structures and topographic features. Rather than refining dynamic grid nesting technique retaining the finite difference scheme we decided instead to adopt finite element technique permitting more flexibility in fitting regular coastline and bathymetry to be fitted with elements of an arbitrary size, shape and orientation (in particular barrier positioning). Considering the importance of setting up a proper model area, three versions of base models are created covering the YS (Yellow Sea and the East China Sea continental shelf), YS/ES (including the Japan and East Sea), YS/ES/NWP (extending to outer east Japanese coast) for focusing the different regions of interest. With this simulator design,

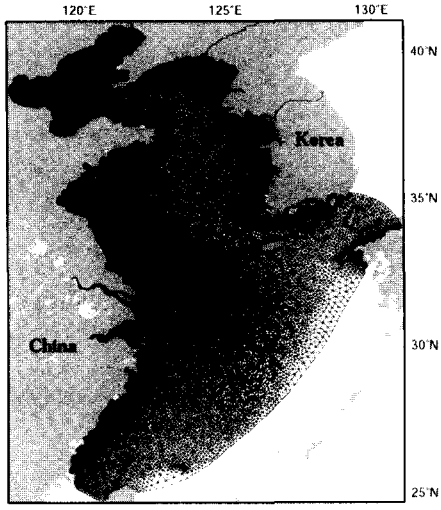

(a)

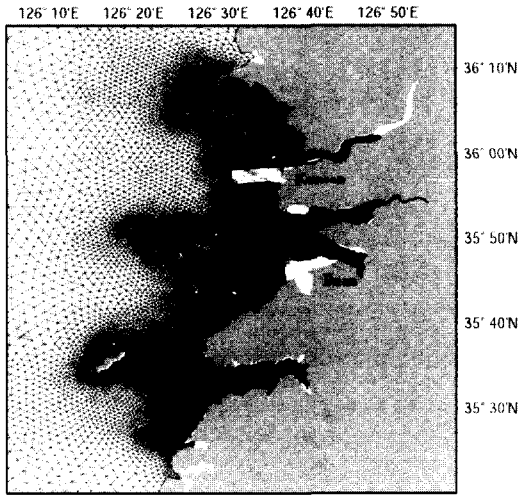

(b)

Fig. 2. Overall mesh and details at the location of Saemangeum barriers.

detailed meshes in the coastal and estuarine regions can be resolved and computations can be manageable with parallel structures, demonstrating easiness of relocatablity within the base model regions. By taking time-stepping approach (Luettich et al., 1992) the method can accommodate the transient response to non-periodic (e.g. wind) forcing in additional to tides contrasting with harmonic approach and can be extended to three-dimensional flow computations subsequently. We have started external mode equations using parametric relationships for bottom friction and momentum dispersion. Key features of the external mode solution include the use of a generalized wave-continuity equation formulation (Lynch and Gray 1979; Kinnmark 1985) using finite element discretizations, details are published widely and will not be restated here

4. Perturbation in tidal current regime

4.1 Residual current at Saemangeum

Evidence of the net residual circulation in the Yellow Sea has not been accumulated so extensively until the deployment of satellite drifting buoys, first during the R/V Thompson and R/V Washington cruise and also by recent numerical models. Changes of tidal residual currents implying tidal circulation in the Yellow Sea have significant effects on transport conditions of suspended sediment. Therefore the deposition environment of fine-grain sand, distribution of various pollutant materials discharged from various sources through the coast, plankton traveling with the tidal current and larvae distribution are all affected by the changes of tidal currents comprehensively. In particular the changes of natural tide system cause the relocation of the tidal front formed along the west coast of Korean peninsula, whichis closely relating to biological communities so that there would be disorders of existing fishing ground.

Besides contribution from tides residual circulation in the Yellow Sea is related with wind forced drift and seasonal thermohaline circulation. The degree of intensity from these forcings is sometimes about similar order and hardly separable especially observed cyclonic gyre in the middle of the Yellow Sea.

Figs. 3 and 5 show the tidal residual currents of M_2 tide before and after dike construction at Saemangeum. The tidal residual currents were easily calculated by time-integrating the modeling results of one periodic M_2 tide before and after dike construction at Saemangeum. The tidal residual currents were easily calculated by time-integrating the modeling results of one periodic M_2 tide. Before dike construction it is found in Figs. 3 and 4 that complicated residual currents due to the bottom topography are dominant at river estuaries and vast tideland. A sizable eddy occurring at near sea between Sinsi and Yami islands before dike construction is seen

in Fig. 4. The simulation model implemented for this study was considering the vast tidal flat at Saemangeum and Geum river estuary, which implies more reasonable and close results of residual currents to the real (Seo and

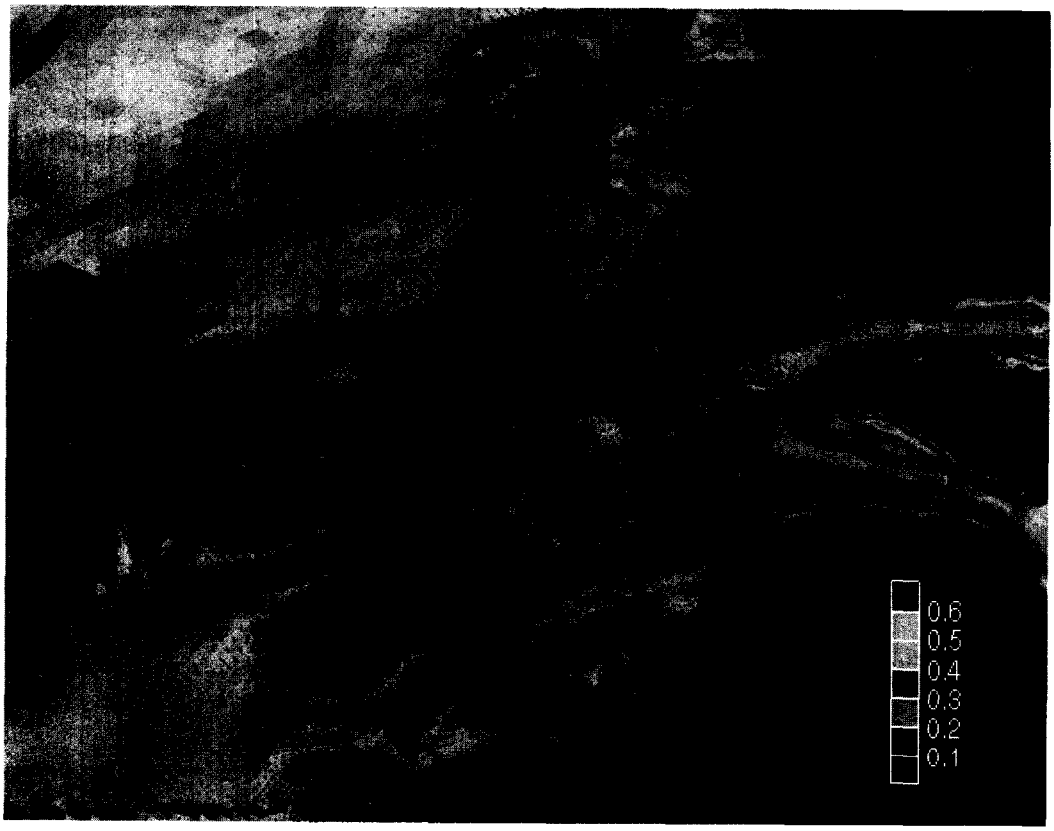

Fig. 3. Tidal residual current before dikes construction (m/s).

Fig. 4. Blow-up of residual currents of Fig. 3 at No. 4 dike (left) and No. 1 and 2 dikes (right) before dikes construction (m/s).

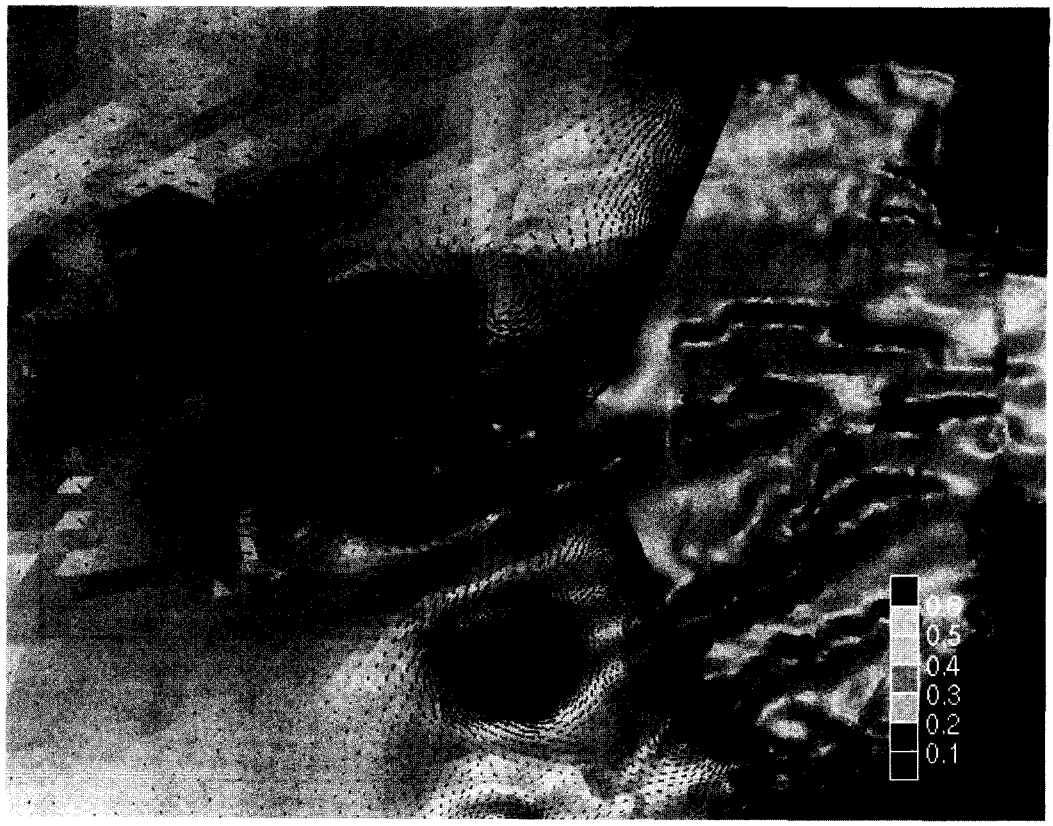

Fig. 5. Tidal residual current after dikes construction (m/s).

Fig. 6. Blow-up ofresidual currents of Fig. 5 at No. 4 dike (left) and No. 1 and 2 dikes (right) before dikes construction (m/s).

Kim, 2003). Residual currents in area of interest are nearly under 10 cm/sec but tidal flats in river estuaries and around islands in both situations. Fig. 6 shows that residual currents with openings completely closed after dike construction contain two large eddies at the both ends of No. 4 dike compared to previous condition without dikes. The lower eddy occurring between Sinsi and Yami islands, where the eddy before dike

construction was found becomes stronger and clearer than before the construction and the other eddy occurs at the point where Kunjang waterway meets the No. 4 dike. It is thought that geographical positions of Kunjang waterway, No. 4 dike and the diagonally located outer barrier may induce the eddy, which eventually causes depositions of fine-grain material by changes of transport conditions of suspended sediment.

4.2 Changes in tidal current characteristics

Changes of the tidal current intensity and major flow direction in Saemangeum tidal regime before and after

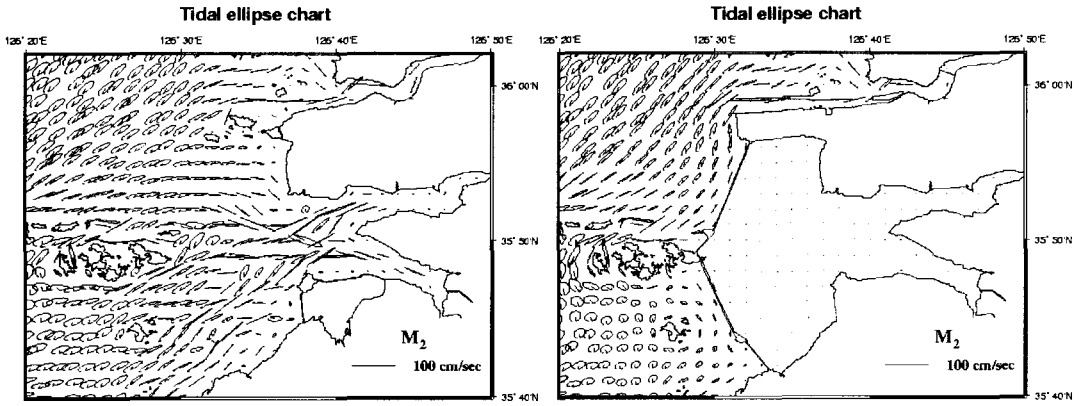

Fig. 7. Tidal ellipse chart of M_2 tide before (left) and after dikes construction (right).

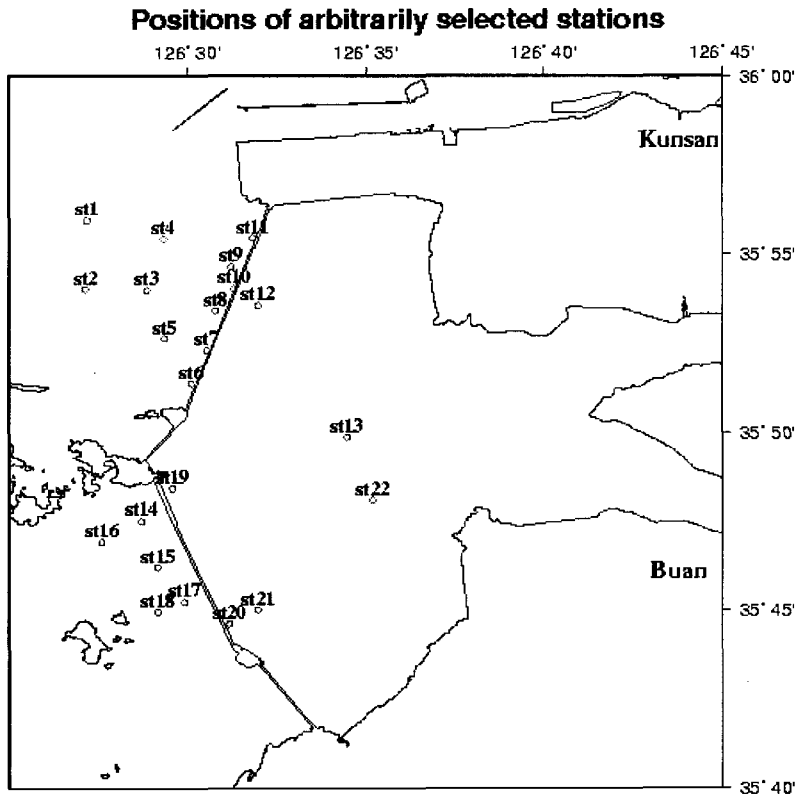

Fig. 8. Positions of selected stations for estimating the changes of tidal current characteristics before and after dikes construction.

dike constructioncan be identified by the changes of tidal ellipse chart and its parameters. Before the dike construction atSaemangeum the rectilinear current movement with small eccentricity at No. 1 and 2 dikes was dominant and became a rotational tidal current with high eccentricity after dike construction. On the other hand the tidal ellipses at No. 4 dike show small changes of eccentricity and spreading trend rather than those at No. 1 and 2 dikes.

Fig. 7 shows the tidal ellipse charts of before and after the dike construction which depict the tidal characteristics and intensities changed. Table. 1 shows the quantitative characteristics of before and after the dike construction with semi-major axis, eccentricity, inclination with positive value indicating a counterclockwise rotation and phase angle. Fig. 8 shows positions of stations selected for comparison of the characteristics.

Figs. 9 to 12show differences of tidal characteristics between before and after Saemangeum dike construction from the results of model simulation. In the whole domain region including Yellow sea tidal regime it is found that the changes of U_{amp}, U_{phs}, V_{amp} and V_{phs} of M_2 tide are not remarkable but Saemangeum area. The characteristics changes of U_{amp}, V_{amp} the dike construction in Saemangeum regime range from 10 cm to 40 cm and range from 0° to 40° for U_{amp}, V_{amp}. At front side of barriers the changes of U_{amp}, V_{amp} are about 20 cm between before and after dike construction. The changing range of tidal characteristics at No. 1 and 2 dikes is distributed toward the open sea further than at No. 4 dike in Saemangeum tidal regime, which thought to be the effect of reductions in the relatively strong tidal current to No. 4 dike by the dikes construction.

Table 1. Comparison of parameters of tidal ellipse chart at selected stations

Station	Before dike constructio				After dike constructio			
	Semi-major axis(m)	Eccentricity	Inclination (deg, +:CCW)	Phase-angle (deg, +:CCW)	Semi-major axis(m)	Eccentricity	Inclination (deg, +:CCW)	Phase-angle (deg, +:CCW)
st1	0.447643995	0.230973	26.7004	116.719002	0.408686012	0.199869	49.5812	122.350998
st2	0.436291993	0.183421	15.5395	108.400002	0.323839992	0.195667	41.0315	115.974998
st3	0.435364008	0.186767	11.5733	106.184998	0.288466007	0.219836	51.8402	119.531998
st4	0.388282001	0.285738	18.6343	107.654999	0.353827	0.199141	65.0894	120.561996
st5	0.471967995	0.174783	10.9049	104.755997	0.252407998	0.161842	50.079	126.926003
st6	0.525960982	0.142961	172.429	269.638	0.178956002	-0.0065315	64.1094	121.880997
st7	0.502987981	0.121174	1.73753	99.3684998	0.238919005	0.00953132	68.7486	129.464996
st8	0.454411	0.1179	4.60994	106.32	0.240787998	0.0465045	69.2113	125.033997
st9	0.397819996	0.138387	6.21402	103.664001	0.287560999	0.0379647	69.9734	118.941002
st10	0.414728999	0.119194	3.84578	105.477997	0.276755005	0.00526886	72.0242	120.781998
st11	0.357672989	0.149382	7.90014	100.814003	0.278131008	0.0120684	72.1951	115.373001
st12	0.424243987	0.0818929	0.248691	106.695999	0.	0.	0.	0.
st13	0.587478995	0.0620772	16.0202	106.537003	0.	0.	0.	0.
st14	0.776805997	0.0407317	24.1199	115.008003	0.077352598	0.170834	164.991	236.074005
st15	0.51036799	0.135006	16.0576	99.3307037	0.149338007	0.29799	130.775	201.923004
st16	0.524582982	0.0945322	26.6775	109.232002	0.112452	0.578841	5.98044	63.0942993
st17	0.477712989	0.162207	15.0786	98.8768005	0.162300006	0.246874	118.844	194.906006
st18	0.343001992	0.134852	5.16768	84.6718979	0.207055002	0.201553	124.249	204.205994
st19	0.817498982	0.0334492	37.1601	120.955002	0.	0.	0.	0.
st20	0.67158097	0.0209056	38.8103	106.314003	0.	0.	0.	0.
st21	0.540699005	0.0921661	23.1858	99.7938995	0.	0.	0.	0.
st22	0.365675986	0.196472	50.2925	112.432999	0.	0.	0.	0.

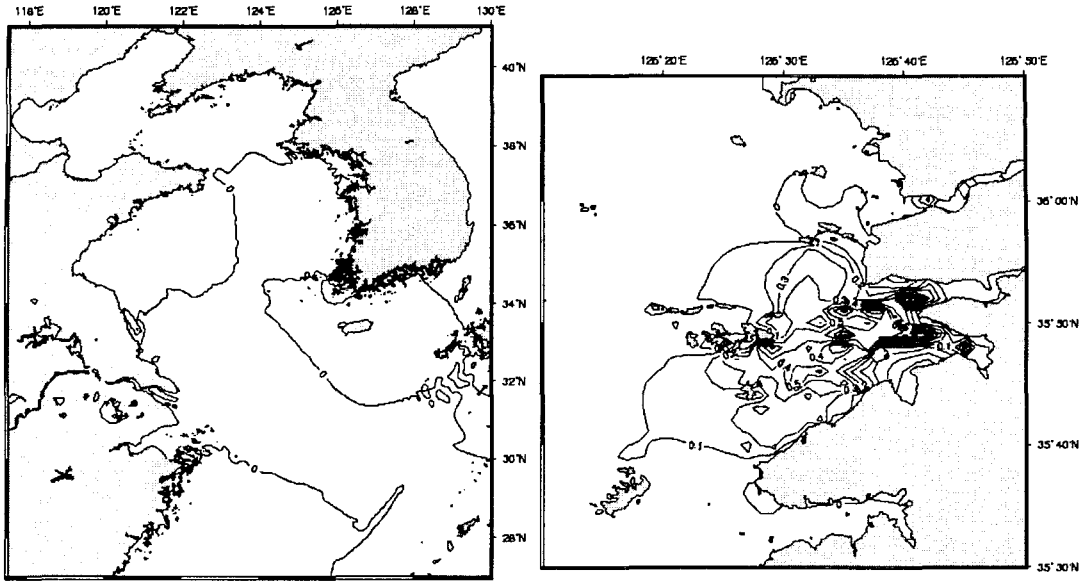

Fig. 9. Changes of U_{amp} of M_2 tide in the Yellow sea (left) and Saemangeum tidal regime (right) between before and after dikes construction (m).

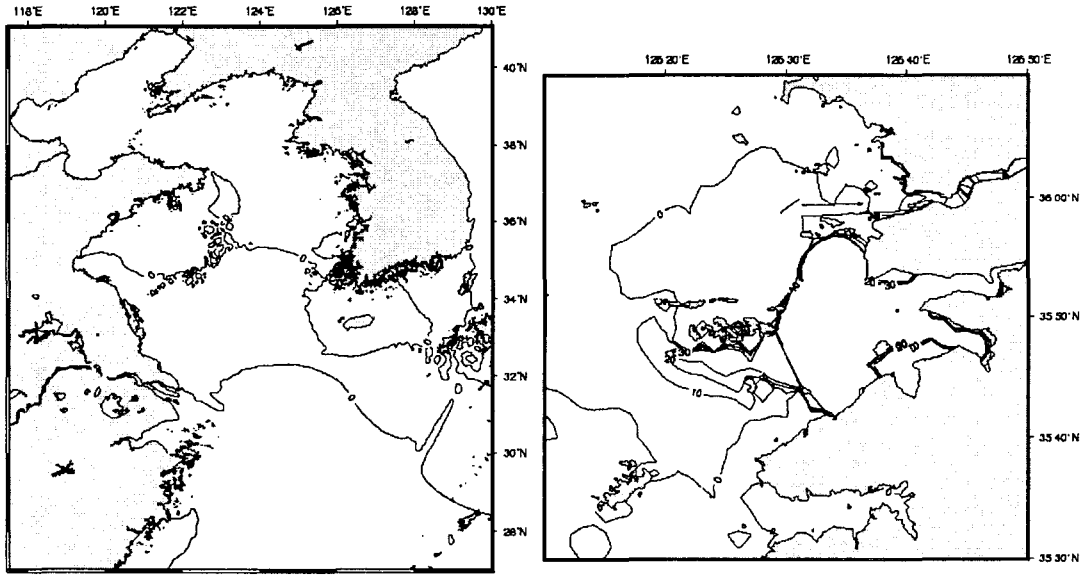

Fig. 10. Changes of U_{phs} of M_2 tide in the Yellow sea (left) and Saemangeum tidal regime (right) between before and after dikes construction (deg).

4.3 Bottom shear stress

The bottom shear stress (τ_b) is a combined effect of currents and waves being induced by the bottom friction which is influenced by bottom roughness. The bottom shear stress which is an index for us to make it possible to evaluate changes and reformation of tidelands was estimated by classical logarithmic resistance law as follows;

$$\tau_b = \frac{1}{2}\rho_w f_c \overline{V}^2 \tag{1}$$

where ρ_w : density of water (kg/m^{-3})

f_c : density of water (kg/m^{-3})

V : depth-averaged velocity (m/s)

Coefficient of the bottom friction (f_c) in Eq. 1 is as follows (Dyer, 1986),

$$f_c = 2\frac{k^2}{\left(\ln\left(30H/k_N - 1\right)\right)}$$

where k : Von Karmann constant (~0.4)

H : water depth (m)

k_N: bottom roughness (m)

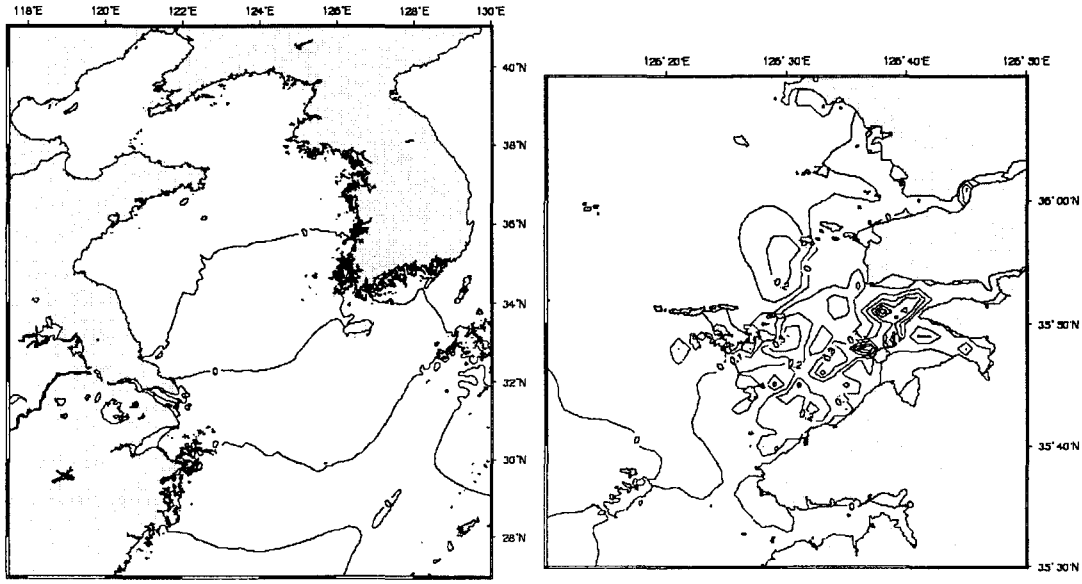

Fig. 11. Changes of V_{amp} of M_2 tide in the Yellow sea (left) and Saemangeum tidal regime (right) between before and after dikes construction (m).

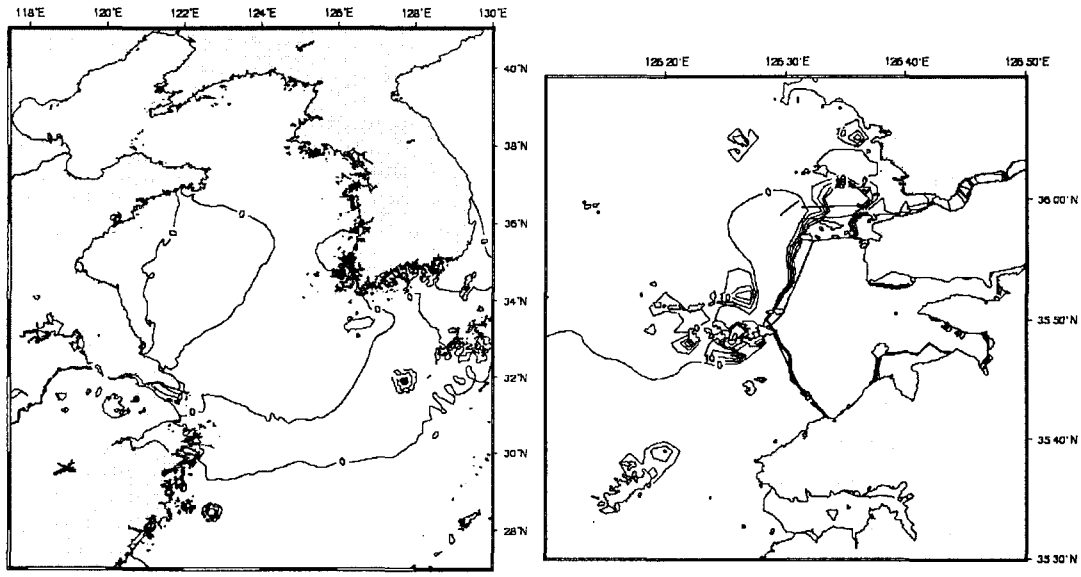

Fig. 12. Changes of V_{phs} of M_2 tide in the Yellow sea (left) and Saemangeum tidal regime (right) between before and after dikes construction (deg).

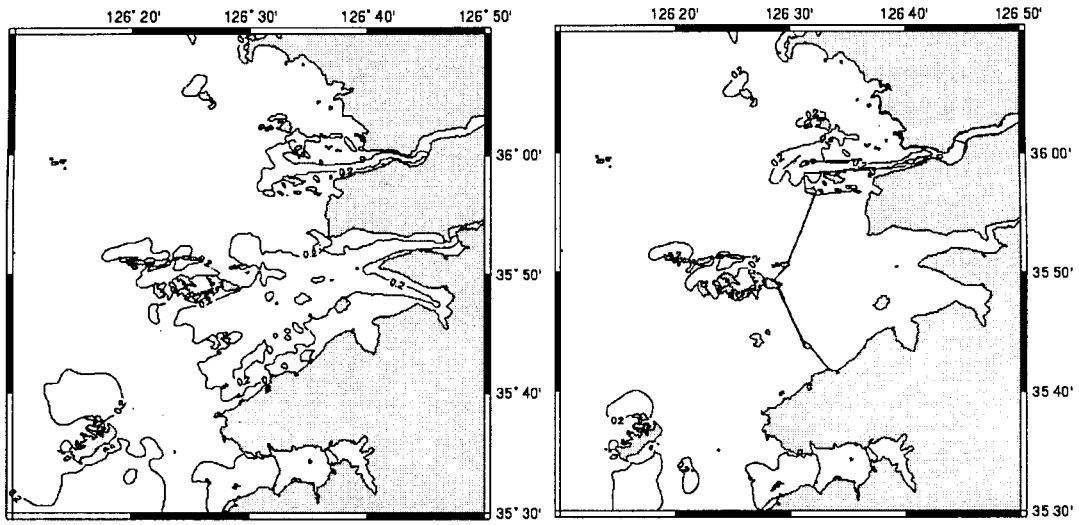

Fig. 13. Bottom shear stress in Saemangeum tidal regime before (left) and after dikes construction (right) (0.2N/m^2).

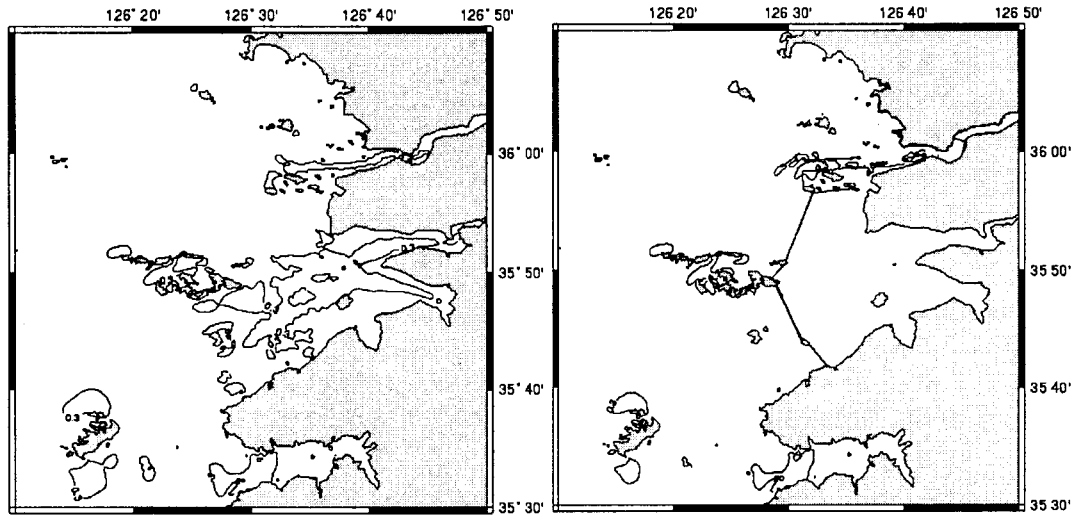

Fig. 14. Bottom shear stress in Saemangeum tidal regime before (left) and after dikes construction (right) (0.3N/m^2).

Figs. 13 and 14 show the bottom shear stress distributions of before and after the dike construction. The 0.3 N/m^2 contour of bottom shear stress before the dike construction is in well agreement with the low tide mark in Saemangeum tidal regime while the 0.3 N/m^2 contour of bottom shear stress after the dike construction does not appear inward from dikes in Saemangeum area. The bottom shear stress contour due to the construction moves toward the open sea outside of dikes. Therefore it is thought to be takena long time to have natural tideland again and some artificial works might be needed to keep the things unchanged.

5. CONCLUSION

The changes of amplitude and phase of 8 constituents and their effects due to the dikes construction in Saemangeum and the Yellow sea tidal regime had been studied (Choi and Lee, 2003). In this study changes of tidal system in Saemangeum and the Yellow sea tidal regime due to the dikes construction has been inquired by considering the changes of various tidal

characteristics.

1. The residual currents at No. 4 dike after the dikes construction have distinct changes showing two eddies at the end of both sides of the dike. It may cause significant depositions of suspended sediments.

2. It is found that the changes of tidal currents after the dikes construction in Saemangeum area have wider range at No. 1 and 2 dikes than No. 4 dike.

3. With the strong rectilinear currents movement changed at No. 1 and 2 dikes the bottom shear stress in Saemangeum area shows similar trend of changes retreating far from river estuaries to the open sea out of barriers. The new natural tidelands after dikes construction may take some time to be reformed.

REFERENCES

Flather, R. A. (1976). A tidal model of the North-West European continental shelf, *Mémoires de la Société Royale des Sciences de Liège, ser.* 6, 10, 141-164.

Choi, B. H. (1978). Computation of barrier effects on tide in Incheon Bay, *Proc. Int. Symp. Korean Tidal Power*, Korean Ocean Res. Development Inst., Seoul, 325-340.

Choi, B. H. (1981). Effect on the M_2 tide of tidal barriers in the west coast of Korea, Korean Ocean Res. Development Inst., Report, 81, 10.

Choi, B. H. (2001). Effect of Saemangeum tidal barriers on the Yellow Sea tidal regime, *Proceedings of the first Asian and Pacific Coastal Engineering Conference, APACE 2001, Dalian, China*, 1, 25-36.

Choi, B. H. and Lee, H. S. (2003). Preoperational simulation of dike construction for Saemangeum tidal regime. *Workshop on Hydro-environmental Impacts ofLarge Coastal Developments*, 91-108.

Garrett, C. and Greenberg, D. A. (1977). Predicting changes in the regime: the open boundary problem, *Journal of Physical Oceanography*, 7, 171-181.

Greenberg, D. A. (1979). A numerical model investigation of tidal phenomena in the Bay of Fundy and Gulf of Marine, *Marine Geodesy*, 2, 161-187.

Heaps, N. S. (1972). Tidal effects due to water generation in the Bristol Channel, 435- 455 *in, Tidal Power, (ed. T. J. Gray and O. K. Gashus), New York: Plenum Press*, 630p.

Heaps, N. S. and Greenberg, D. A. (1974). Mathematical model studies of tidal behavior in the Bay of Fundy, *Proc. IEEE International Conference of Engineering in the Ocean Environment, 1, 388-389. New York: Institute of Electrical and Electronic Engineers*, 399 and 318p.

Huthnance, J. M. (1982). On one mechanism forming linear sand banks. *Estuarine, Coastaland Shelf Science*, 1,89-99.

Garrett, C. (1972). Tidal resonance in the Bay of Fundy and Gulf of Maine, *Nature*, 238p, 441-443.

Duff, G. F. D. (1979). Numerical modelling of tides in the Bay of Fundy, 93-98 *in Tidal Power and estuary management, (ed. R. T. Severn, D. L. Dineley and L. E. Hawker), Bristol: Scientechnica*, 296p, (*Colston Paper* No. 30).

Luettich, R. A., Westerink, J. J. and Scheffner, N. W. (1992). ADCIRC: An advanced three-dimensional circulation model for shelves, coasts, and estuaries, report 1: theory and methodology of ADCIRC-2DDI and ADCIRC-3DL, *Dredging Research Program Technical Report DRP-92-6, U.S. Army Engineers*, Waterways Experiments Stations, Vicksburg, MS, 137p.

Lynch, D. R. and Gray, W. G. (1979). A wave equation model for finite element tidal computations, *Computers and Fluids*, 7, 207-228.

Kinnmark, I. P. E. (1985). The shallow water wave equations: formulation, analysis and application, *Lecture Notes in Engineering*, 15, 187p.

Seo, S. W. and Kim, J. H. (2003). Comparative study for dry-wet treatment effect in a tidal hydrodynamic simulation. *Journal of Korean Society of Coastal and Ocean Engineers*, 2, 97-107